AD-A071 188 CONTROL DATA CORP MELVILLE N Y TRG DIV F/G 17/1
TWO ARRAYS ON A WEDGE,(U)
JUN 66 V MANGULIS, J GOBINS
UNCLASSIFIED TRG-023-TM-66-28 NOBSR-93023
NL

| OF |
AD
A071188

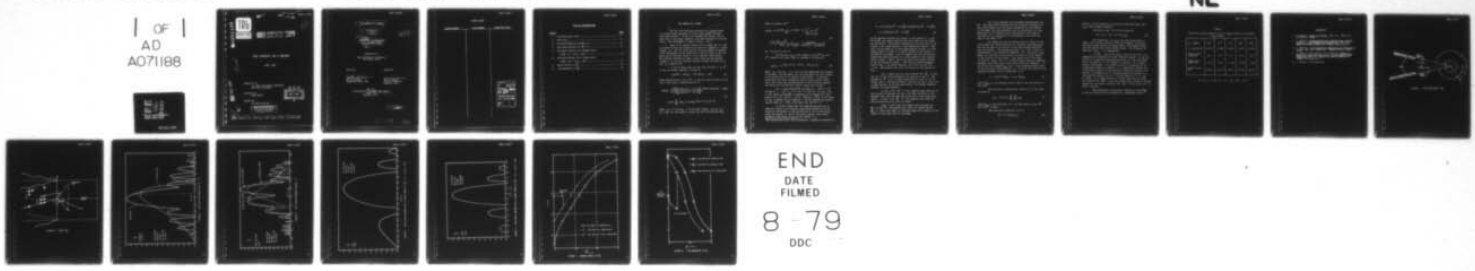

END
DATE FILMED
8-79
DDC

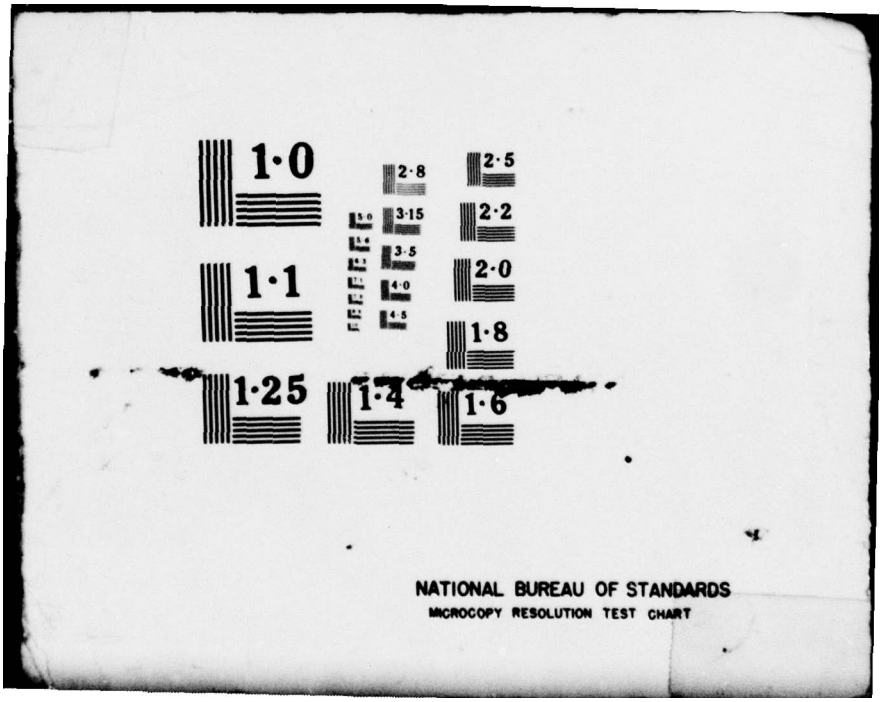
1·0
1·1
1·25
2·8
3·15
3·5
4·0
4·5
1·4
2·5
2·2
2·0
1·8
1·6
NATIONAL BUREAU OF STANDARDS
MICROCOPY RESOLUTION TEST CHART

TWO ARRAYS ON A WEDGE

JUNE 1966

SUBMITTED TO:

U. S. NAVY ELECTRONICS LABORATORY
SAN DIEGO, CALIFORNIA

CONTRACT NO.:

NObsr-93023

REPORT NO.:

TRG-023-TM-66-28

TRG / A SUBSIDIARY OF CONTROL DATA CORPORATION
ROUTE 110 • MELVILLE, NEW YORK 11749 • 516/531-0600

WP22-1-42010

(6) TWO ARRAYS ON A WEDGE,

(10) V./ Mangulis
J./ Gobins

(12) 19p.

(14) TRG-
Report No. 023-TM-66-28
Contract NObsr-93023
(15)

Submitted to:

Navy Electronics Laboratory
San Diego, Calif.

Approved:

Walton Graham
Walton Graham,
Department Head, TRG

Approved:

Marvin Baldwin
Project Technical
Director, NEL

TRG, Inc.
A Subsidiary of Control Data Corp.
Route 110
Melville, N.Y.

TRG DIV.

(11) June 1966

353 415

CHANGE SHEET

CHANGE NUMBER	PAGE NUMBER	EFFECTIVE DATE

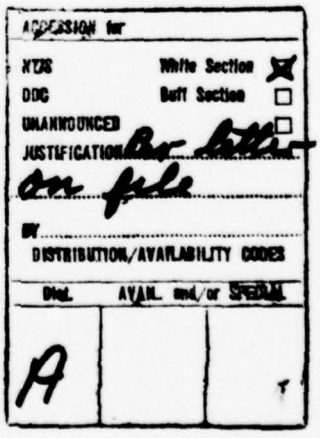

LIST OF ILLUSTRATIONS

TWO ARRAYS ON A WEDGE

The far field radiation pattern for a phased array on a rigid corner or wedge of corner angle $\psi > 180°$ has been calculated before.[1] We will now consider two arrays, one on each side of the wedge, phased to the same direction in the far field. The arrangement is shown in Figs. 1 and 2.

Each of the arrays consists of N columns and M rows of elements which are assumed to be small as compared to a wavelength, i.e., the far field pattern of each element is assumed to be independent of the direction to the far field if the elements are in the free field or in an infinite rigid baffle. The distance between the edge of the corner and the nearest column is w, and the spacings between columns and rows are d_1 and d_2, respectively.

It can be shown that the far field pattern at θ, ϕ^* of the two arrays together is given by

$$E_2(\theta,\phi^*) = E(\theta,\tfrac{1}{2}\psi - \phi^*) + E(\theta,\tfrac{1}{2}\psi + \phi^*), \qquad (1)$$

where $E(\theta,\phi)$ with $\phi = \frac{1}{2}\psi \pm \phi^*$ is the far field pattern of just one of the arrays, obtained before as[1]

$$E(\theta,\phi) = \frac{\sin\left[\frac{1}{2} M\, kd_2(\cos\theta - \cos\theta_o)\right]}{M \sin\left[\frac{1}{2} kd_2(\cos\theta - \cos\theta_o)\right]} e^{\frac{1}{2}i(M-1)kd_2(\cos\theta - \cos\theta_o)} \qquad (2)$$

$$\times (1/N) \sum_{n=1}^{N} S(kx_n \sin\theta,\phi) e^{-ikx_n \sin\theta_o \cos\phi_o}$$

where $x_n = w + (n-1)d_1$, k is the wave number, θ_o and $\phi_o = \frac{1}{2}\psi \pm \phi_o^*$ are the angles to which the far field pattern main

beam is steered, and*

$$S(u,\phi) = e^{iu\cos\phi} - \frac{1}{\sqrt{\pi}} e^{iu\cos\phi} + i\frac{\pi}{4}\int_{\sqrt{2u}\cos\frac{1}{2}\phi}^{\infty} ds\, e^{-is^2}$$

$$+ \frac{e^{-iu - i\frac{\pi}{4}}}{\psi}\left(\frac{\pi}{2u}\right)^{\frac{1}{2}}\left[\frac{\psi}{2\pi\cos\frac{1}{2}\phi} + \frac{\sin(\pi^2/\psi)}{\cos(\pi^2/\psi) - \cos(\pi\phi/\psi)}\right] \qquad (3)$$

for $kw \sin\theta >> 1$ and $\psi > \pi$.

The velocity v_{nm} of the element in the m^{th} row and n^{th} column of the sonar array is assumed to be given by

$$v_{nm}/v_{11} = e^{-ikx_n \sin\theta_o \cos\phi_o - ikz_m \cos\theta_o} \qquad (4)$$

where $z_m = (m-1)d_2$, i.e., the velocity magnitudes are assumed to be equal, and the phases are the same which one would choose if the array were on an infinite plane baffle. It has been shown that the latter assumption yields results which differ very little from the optimum pattern in which velocity phases are chosen with diffraction effects taken into account.[1]

Fig. 3 shows $\left|E_2(\theta,\phi^*)\right|$ and $\left|E(\theta, \frac{1}{2}\psi - \phi^*)\right|$ vs. ϕ^* for $\phi_o^* = 0°$, $\psi = 352°$, $\theta_o = \theta = 90°$, N = 229, M = 12, $kd_1 = kd_2 = 2.09$, which corresponds to spacings of 0.2 meters at a frequency of 2.5 kc, and kw = 114.39. $\left|E(\theta,\frac{1}{2}\psi + \phi^*)\right|$ is not shown in Fig. 3 because due to symmetry it can be obtained by reflecting the $\left|E(\theta, \frac{1}{2}\psi - \phi^*)\right|$ curve about the line $\phi^* = 0°$.

It is well known that the composite pattern of two identical arrays on an infinite rigid plane baffle can be obtained as the product of the pattern due to one of the arrays times the pattern B due to two point sources, each source located at the center of one of the arrays, i.e.,

*The second term in Eq. (3) of Reference 1 should be divided by π.

$$B = \sin\left[kL(\sin\phi^* - \sin\phi_o^*)\right]/\sin\left[\tfrac{1}{2}kL(\sin\phi^* - \sin\phi_o^*)\right]$$

$$= 2\cos\left[\tfrac{1}{2}kL(\sin\phi^* - \sin\phi_o^*)\right] \qquad (5)$$

if the distance between the centers of the arrays is L, and ϕ^* and ϕ_o^* are angles measured from the normal to the arrays and the baffle. The product theorem will not hold for our two arrays on the wedge because of the diffraction effects. However, we can expect it to hold approximately in Fig. 3 in the narrow region $-4° \leq \phi^* \leq 4°$ in which neither of the arrays is shielded by the wedge. One can imagine that the two end-fire arrays have been projected on a plane normal to the bisector plane in Figs. 1 and 2, and we can apply the product theorem to the two projected arrays. Then for the array parameters used in Fig. 3. we obtain from Eq. (5) a null in B at $\phi^* = \pm 3.6°$, which agrees well with the minima in the pattern in Fig. 3.

Fig. 4 shows the far field patterns for $\phi_o^* = 4°$ and the rest of the array parameters the same as in Fig. 3. The minimum at $\phi^* = 0.4°$ is again explained by a null in B; of course, due to diffraction effects one does not get a true null in $|E_2|$ because, as we mentioned before, the product theorem applies only approximately.

In Fig. 3 for $\phi_o^* = 0°$ the composite main beam due to both arrays is narrower (at the -6 db level relative to the maximum, say) than the main beam from each of the arrays separately. In Fig. 4 for $\phi_o^* = 4°$ the composite main beam has been practically split into two beams.

Figs. 5 and 6 show the single array patterns for $\phi_o^* = 8°$ and 16°; the second array cannot be steered beyond $\phi_o^* = 4°$ since that angle is a grazing angle with respect to the baffle of the other side of the wedge.

Let us now consider the cavitation limited power output. The near field pressures and the radiation impedances of the array elements are relatively unaffected by the presence of the wedge, and such quantities can be calculated as if the array were on an infinite plane rigid baffle if the edge of the array is at a distance of a wavelength or more from the edge of the wedge.[2,3,4]

For simplicity one can assume that the ratios of the actual peak near field pressures for different steering angles will be the same as the ratios of the peak average pressures over the pistons. The average pressure p_{av} over a piston is proportional to the radiation impedance, i.e., the force $p_{av}A$, where A is the area of the piston, is equal to $v\rho cAZ$, where v is the velocity of the piston, ρ the density and c the speed of sound in water, and Z is a dimensionless radiation impedance parameter such that ρcAZ is the actual radiation impedance. If we now set the maximum $|p_{av}|$ (for a fixed steering angle) equal to the cavitation limit pressure p_c, we obtain the value of the maximum allowable velocity amplitude v_c as

$$v_c = p_c A/\rho cA \; |Z|_{max} = p_c/\rho c \; |Z|_{max} \tag{6}$$

where $|Z|_{max}$ is the maximum value of $|Z|$ of all the pistons in the array.

The cavitation limited power output out of the array is given by

$$P_{out} = \frac{1}{2} v_c^2 \; \rho cA \sum_{m=1}^{M} \sum_{n=1}^{N} R_{mn} \tag{7}$$

where R_{mn} is the real part of Z for the piston in the m^{th} row and n^{th} column.

The directivity index DI in db is

$$DI = 10 \log(I_o/I_{av}) \tag{8}$$

where I_o is the intensity on the axis of the main beam, and I_{av} is the average intensity.

The source level SL in db is given by

$$SL = 71.6 + DI + 10 \log (P_{out}) \qquad (9)$$

The quantities v_c, P_{out}, DI, and SL are given in Table I for a single array of 12 by 229 elements, with both rows and columns spaced 0.2 meters apart, the elements being circular pistons with radii 0.0635 meters. The frequency is 2500 cps, and p_c = 1.5 atmospheres.

In Figs. 7 and 8 the source levels SL and the 3 -db beamwidths are compared for three different arrays: 1) the two arrays on a wedge as discussed previously, so that the arrays are at an angle of 4° with respect to endfire; 2) a single array on the wedge; 3) a single array on a halfplane not inclined with respect to endfire, i.e., diffraction effects due to the finite extent of the baffle are taken into account, but endfire is assumed to be at a grazing angle with respect to the array and baffle, not at 4° off the baffle as in 1) and 2) above. In 1) above one has to assume that only one array will operate for $\phi_o^* > 4°$, since the second array cannot be steered behind its own baffle; therefore for $\phi_o^* = 4°$ the curves for 1) and 2) coincide.

The implication of the above results for the design of the C/P array will be discussed in a subsequent report.[5]

TABLE I

Cavitation Limited Quantities for a Single Array on an Infinite Plane Baffle

ϕ_o, degrees	180°	176°	172°	168°	160°
v_c, meters/sec	0.0235	0.0228	0.0305	0.0431	0.0778
Power output, kilowatts	20.3	25.3	50.7	67.9	132.2
Directivity index, db	29.35	28.17	27.66	29.38	31.63
Source level, db	144.03	143.79	146.31	149.30	154.44

$M = 12$, $N = 229$, $\theta_o = 0°$, $kd_1 = kd_2 = 2.09$.

REFERENCES

1. V. Mangulis, Array on a Corner, TRG, Inc., Report No. 023-TN-66-1 (1966).

2. V. Mangulis, Baffle Reflections, Diffraction, and Non-rigidity in the CONTACT Sonar System (U), TRG, Inc., Report No. TRG-011-Memo-64-1 (1964); (Confidential).

3. V. Mangulis, On the Radiation Impedance of a Piston on a Corner, TRG, Inc., Report No. TRG-023-TN-65-2 (1965).

4. A. Kane, T. De Filippis, and V. Mangulis, Effect of Reflections from the Ship's Hull on the CONTACT Sonar Array (U), TRG, Inc., Report No. TRG-023-Memo-65-2 (1965); (Confidential).

5. A. Novick, to be published.

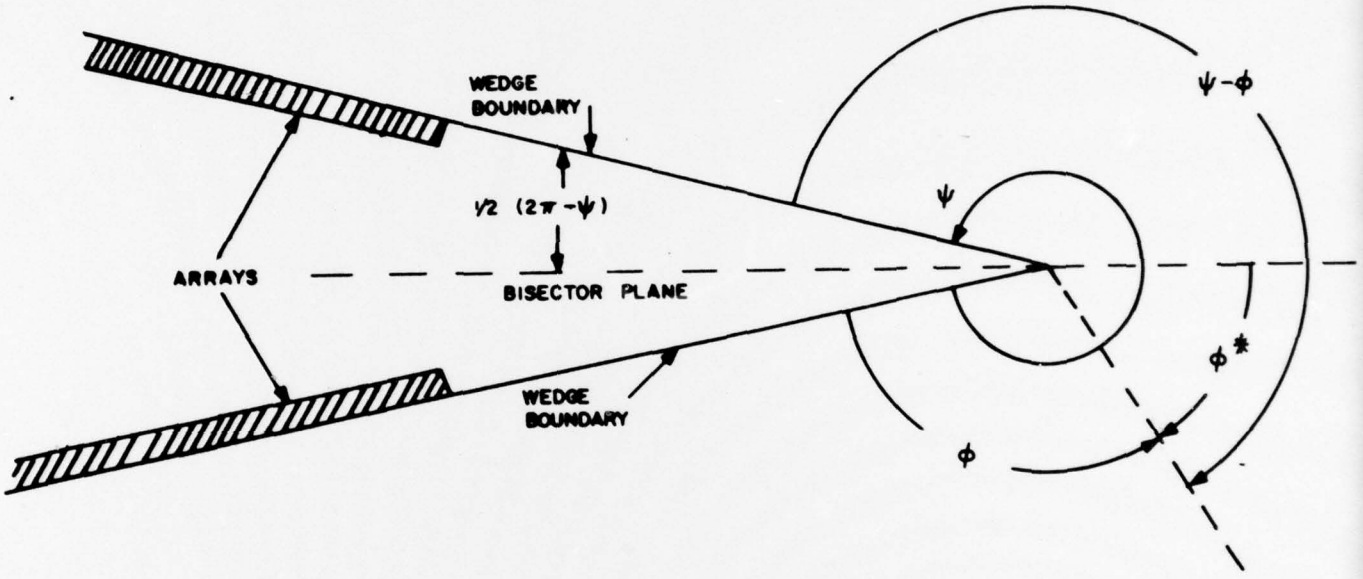

FIGURE I. CROSS-SECTIONAL VIEW

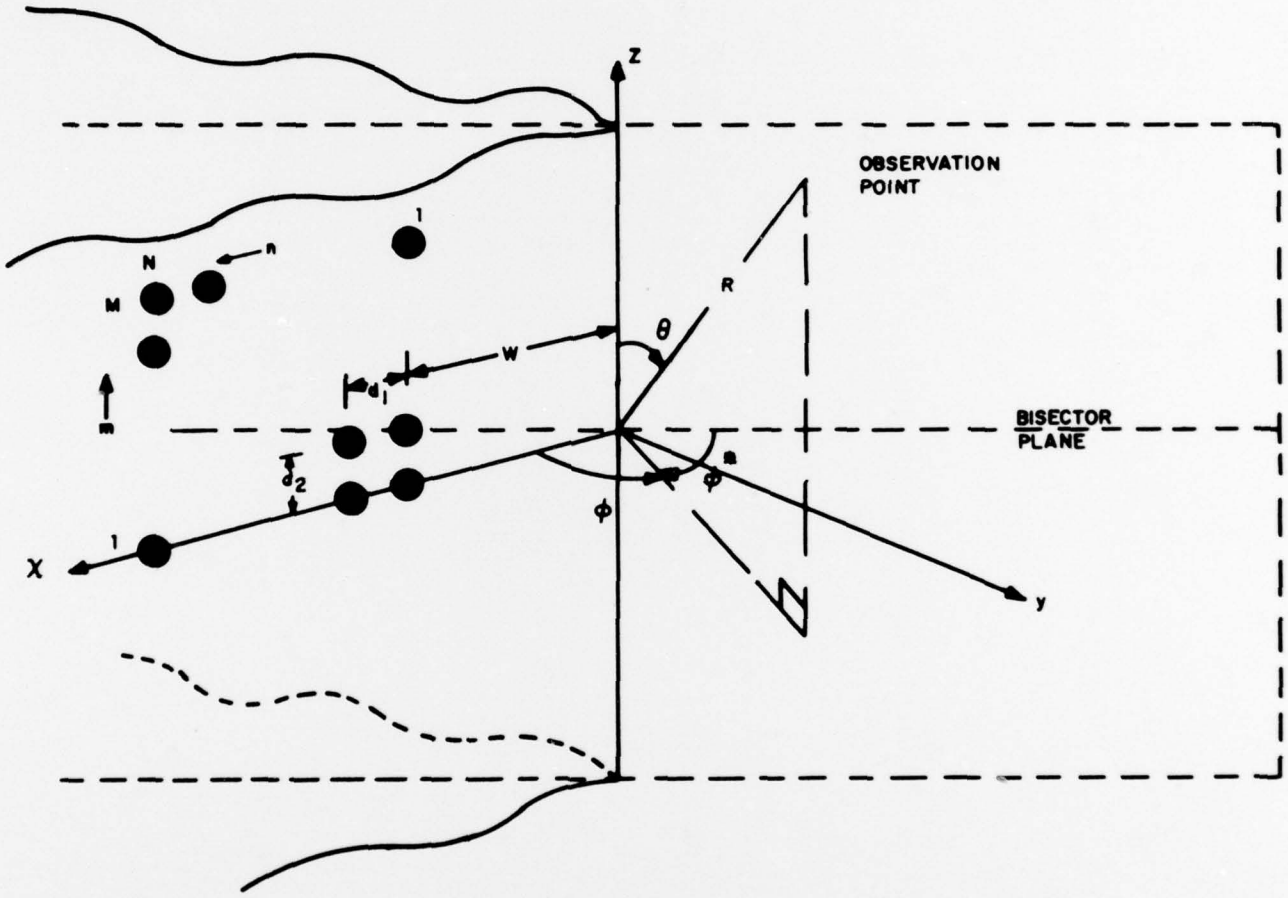

FIGURE 2. SIDE VIEW

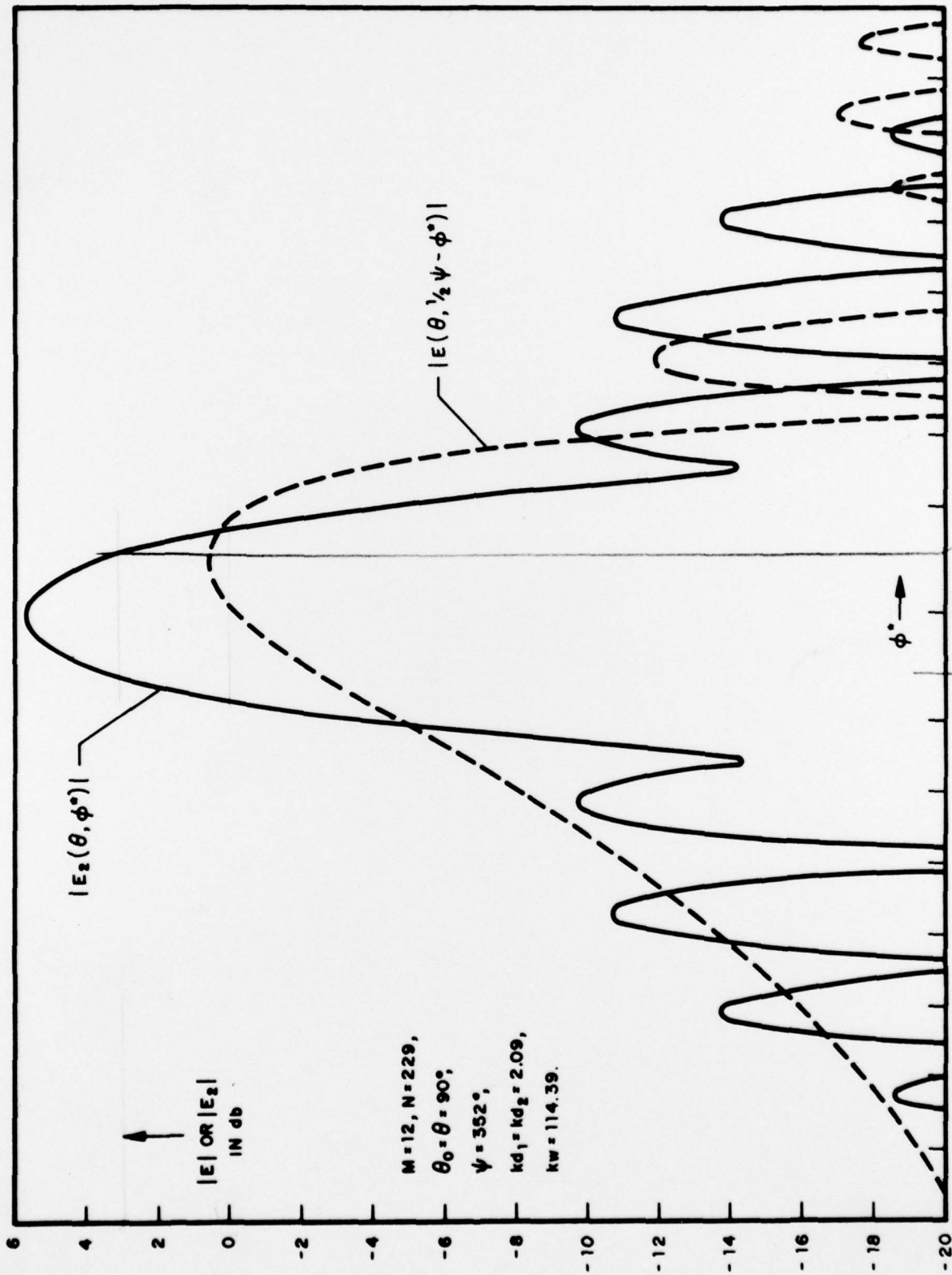

FIGURE 3. FAR-FIELD PATTERNS FOR $\phi_o^* = 0°$

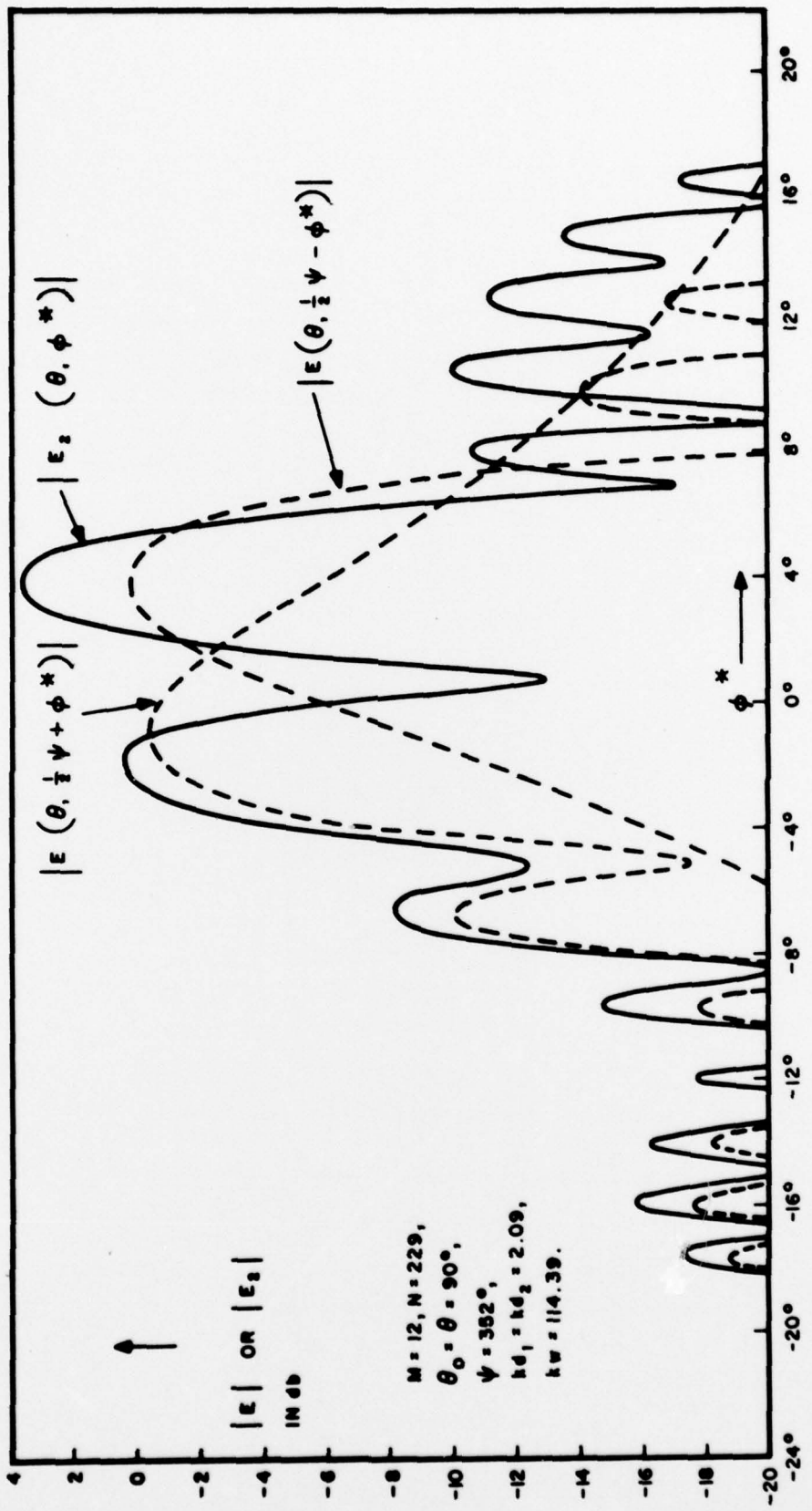

FIGURE 4. FAR-FIELD PATTERNS FOR $\phi_o^* = 4°$

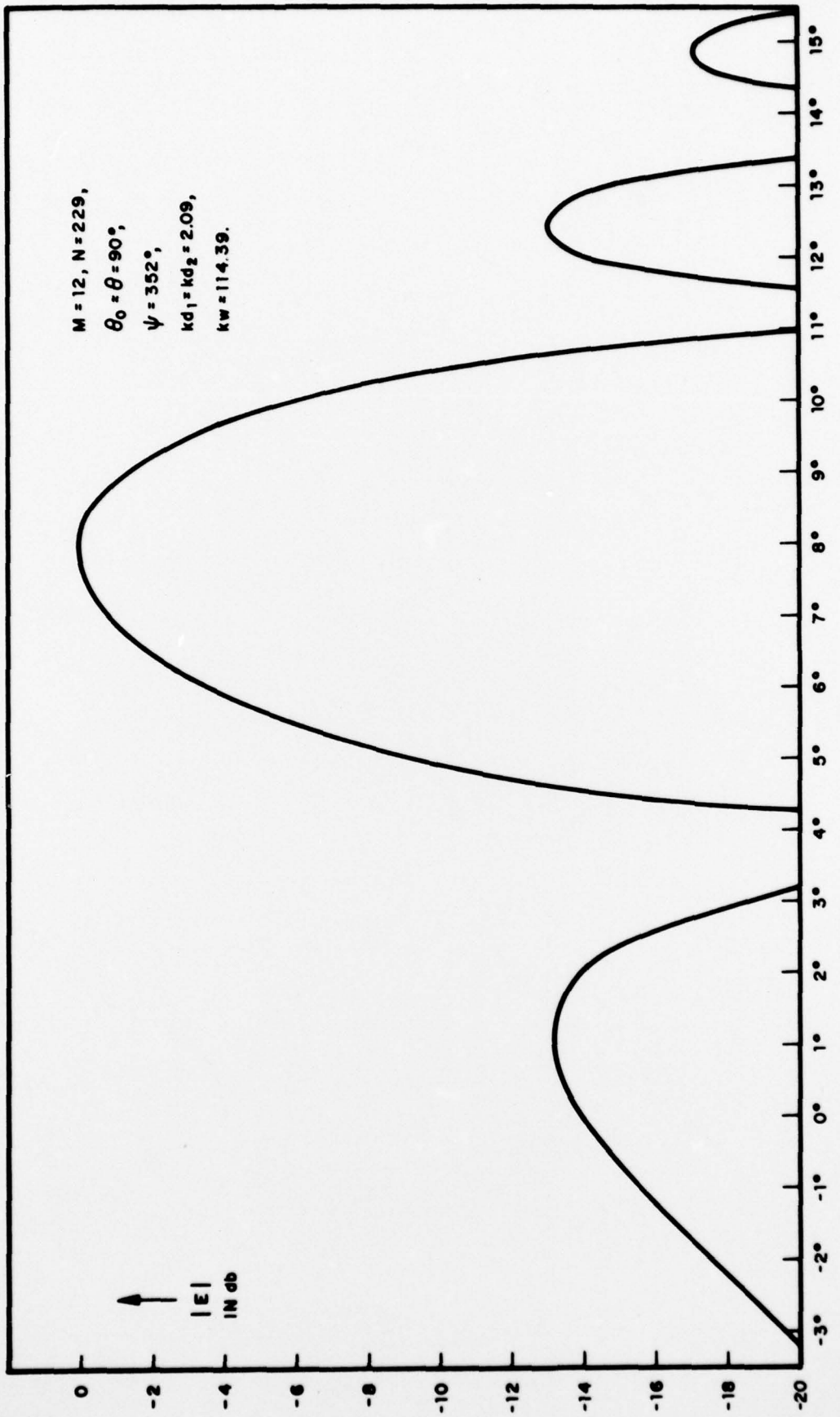

FIGURE 5. FAR-FIELD PATTERN FOR A SINGLE ARRAY AT $\phi_o^* = 8°$, or $\phi_o = 168°$

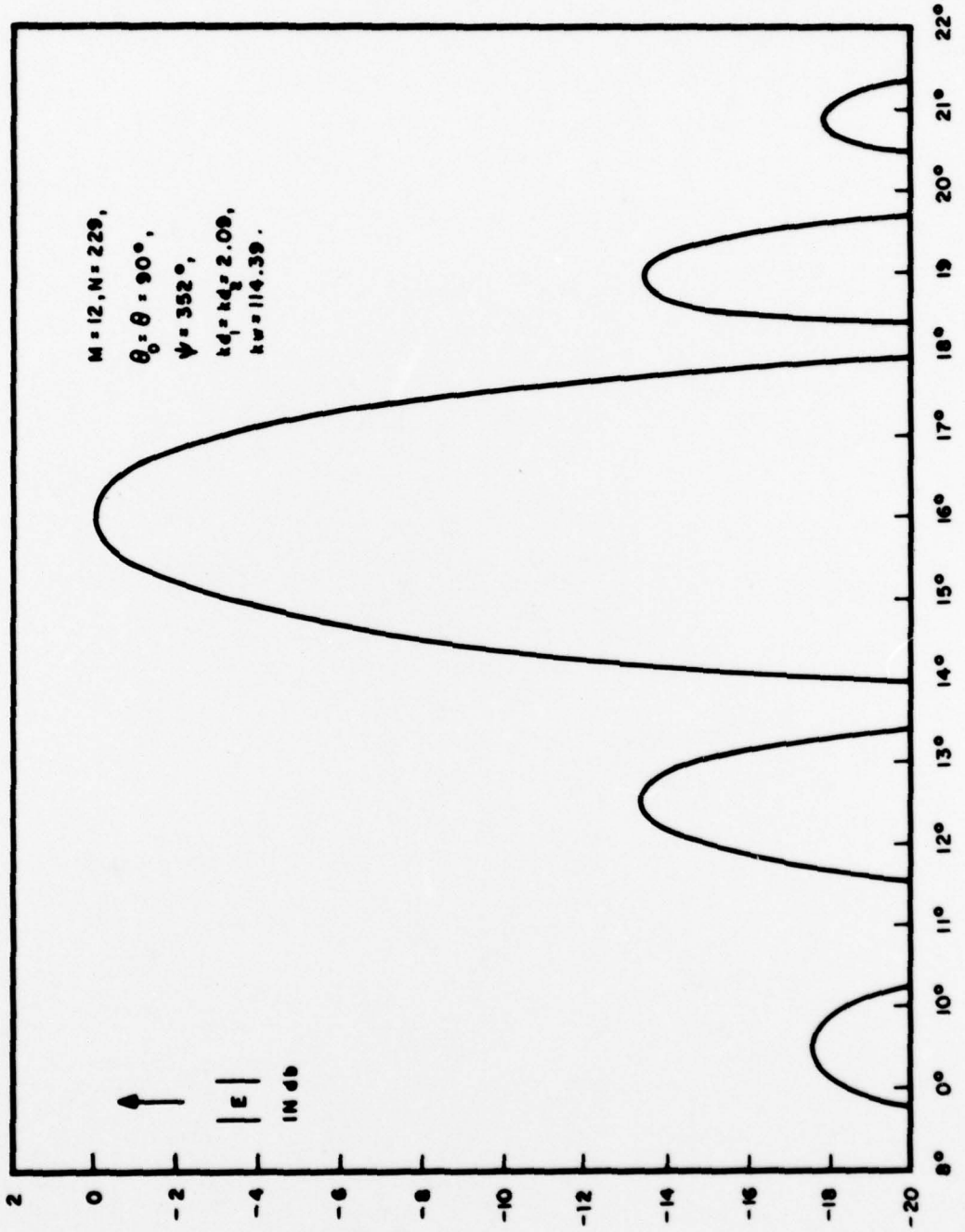

FIGURE 6. FAR-FIELD PATTERN FOR A SINGLE ARRAY AT $\phi_o^* = 16°$, or $\phi_o = 160°$

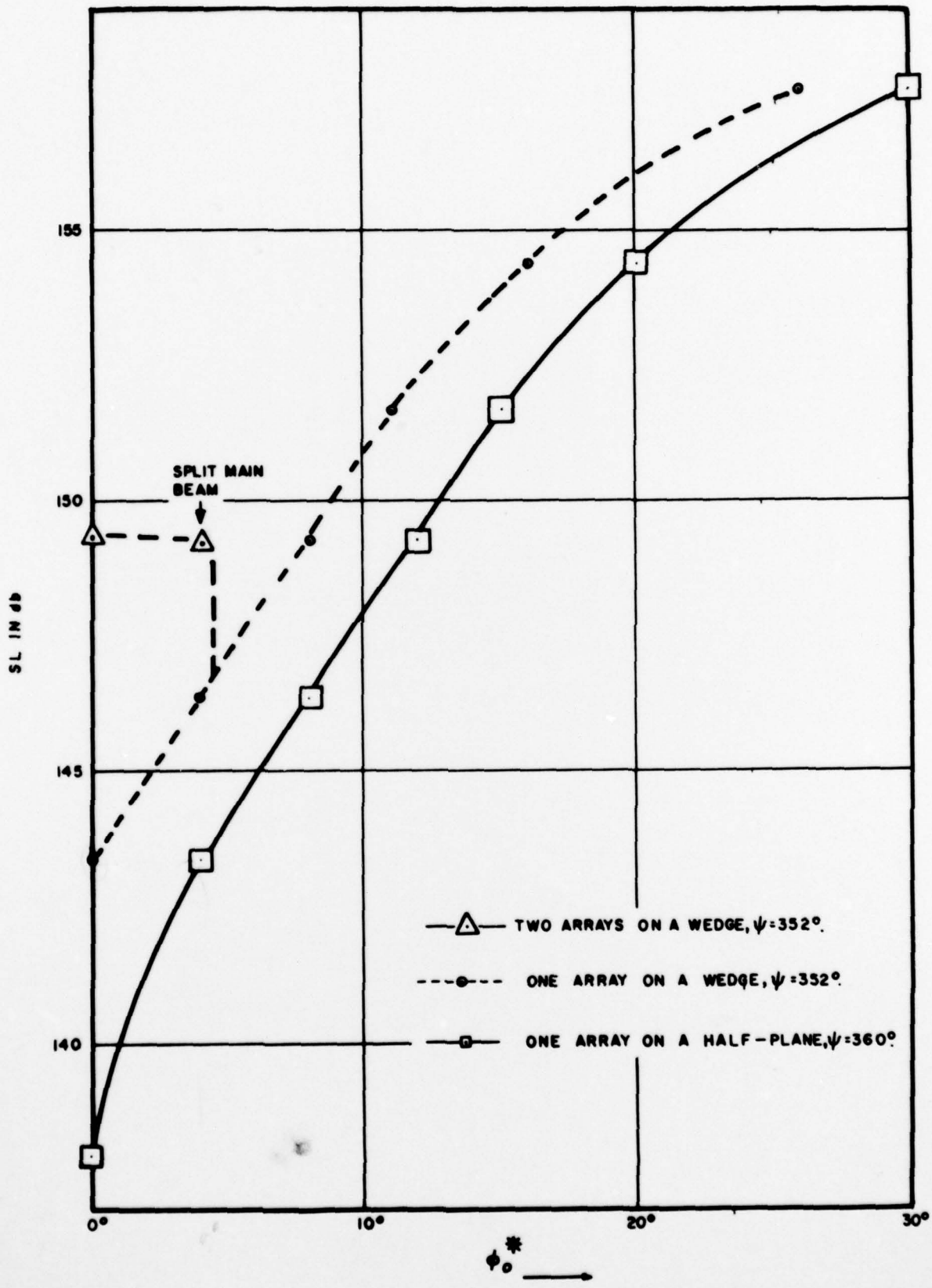

FIGURE 7. SOURCE LEVELS VS ϕ_o^*

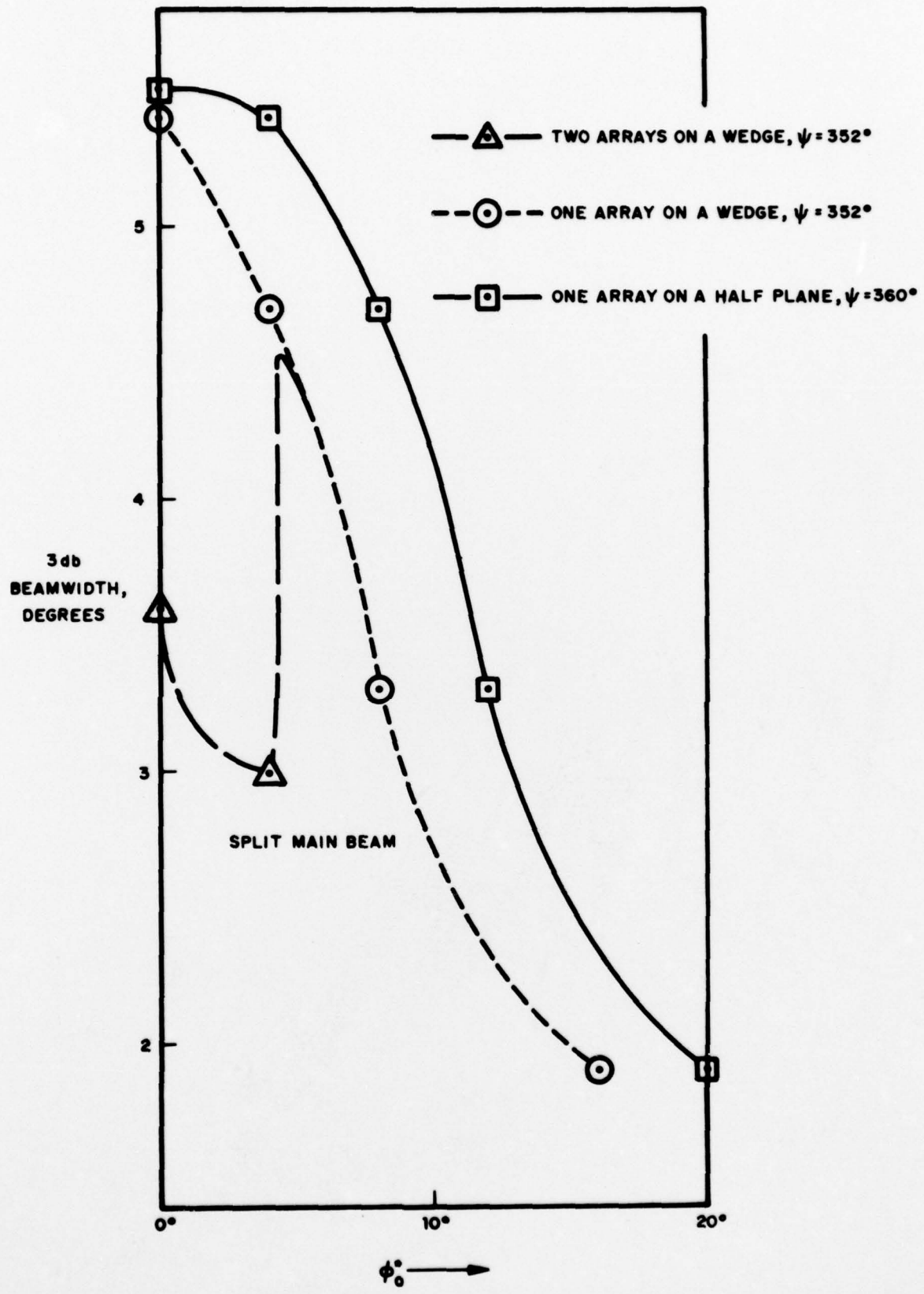

FIGURE 8. 3 DB BEAMWIDTH VS ϕ_o^*